Autonomous Unmanned Aerial Vehicles for Examining Current and Evolving Distribution of Contamination from the FDNPP Accident - 17020

Peter G. Martin *, Y. Yamashiki **, Thomas B. Scott *, Oliver D. Payton *,
David A. Richards *, and John S. Fardoulis *
* University of Bristol, United Kingdom, BS8 1TH
** University of Kyoto, Japan, 606-8501

ABSTRACT

Estimates as well as subsequent measurements of the radiation released following the events at the Fukushima Daiichi Nuclear Power Plant in March 2011 place the incident as the second greatest nuclear event to have ever occurred – duly rated at the maximum of Level 7 on the INES Event Scale. The releases of radioactivity from the plant were detected worldwide, however the multi-reactor nature of the events at the FDNPP has complicated the understanding of the radionuclide release inventory and the subsequent distribution of the material.

As a result of this highly-complex release scenario, it is important to understand the current and evolving state of contamination within the rapidly evolving, topographically extreme and frequently typhoon impacted environment on Japan's eastern coast.

Existing systems rely either on high-altitude manned aircraft to perform such contamination surveys, correcting results to ground-level, or, on humans manually measuring the dose-rate on foot. In order to overcome the shortcomings of both methods, a low-altitude unmanned aerial vehicle (UAV) has been developed at the University of Bristol and successfully deployed to the affected areas surrounding the FDNPP. In contrast to these other methods; the use of low-altitude UAVs provides a spatial resolution previously achievable only through the deployment of humans on the ground, with the potential for significant radiation exposure. This high-resolution monitoring allows for subsequent modelling to inform our understanding of the behaviour and long-term stability of the fallout material.

INTRODUCTION

Contamination Release

On the 11th March 2011, a 15 m high tsunami initiated by the magnitude 9.0 Great Tohoku Earthquake off the eastern coast of Japan, caused the loss of coolant incident (LOCI) at the Fukushima Daiichi Nuclear Power Plant (FDNPP). Over the 12 days succeeding the tsunami, a series of large explosions occurred on the multiple-reactor site culminating in the release of a considerable amount of radioactive material. This radioactive release was estimated to be approximately 10% of the total activity (520 PBq) of that produced by the Chernobyl accident (5300 PBq – excluding noble gases) twenty-five years previously [1]. Despite representing only 10% of the total activity released, the Fukushima release comprised a greater proportion of the highly-volatile yet short-lived noble gases (Kr-85 and Xe-133). Unlike the earlier Chernobyl release

also – whereby the contamination was predominantly dispersed over land (detected throughout the majority of the European continent by numerous groups [2–5], the contamination released following the incident in Japan was largely directed out into the neighbouring Pacific Ocean, with only 20% moving westwards – falling on land. The steeply mountainous topography of the region and the moist atmospheric conditions at the time of the incident were both highly influential in the concentrated deposition of this landward contamination within the areas north-west trending valleys – preventing the wider spread of the highly-active material.

The devastating nature of the combined earthquake and tsunami on the area meant that as well as the external power supplies feeding the nuclear plant being destroyed, the radiation monitoring network that surrounded the plant was also removed. With no accurate means by which to monitor the initial and evolving spread of radioactivity in the environment following the explosive events at the plant, a number of arbitrary exclusion zones were emplaced and evacuation zones setup based on only a limited number of surviving monitoring points. It was not until 6 days after the event that the first survey to monitor the contamination was made through the deployment of manned helicopter and fixed-wing survey flights, with results published 5 days later.

High-Altitude Monitoring

As a collaboration with the US DoE, the Japanese Ministry of the Education, Culture, Sports, Science and Technology-Japan (MEXT) performed the above mentioned series of survey flights across the 80 km region extending north-west from the crippled nuclear site. These missions allowed a crude insight into not only the distribution of radioactive material, but also the species present. Following this work, refinement of exclusion and evacuation zones was made.

Despite providing insight into contamination, the on-ground resolution attained via these systems was comparatively low. Consisting of C12 and UK-1 aerial vehicles equipped with 16 x 4 x 2” NaI detectors, flying at typical altitudes of 400 m (150 – 700 m); following a three-hour duration flight, a total of over one thousand radiation measurements were attained covering a comparatively large area outwards from the plant. Although representing the collection of data from the largest area, the resolution at which it is attained is low and highly costly in comparison to other survey methods. Further additional disadvantages of this survey method are the significant dose those on-board the helicopter could receive whilst performing the survey, and also the contamination of an expensive asset due to the plume through which the vehicle would likely be travelling.

Ground Monitoring

In contrast to the high-altitude surveys conducted initially as part of the US DoE and MEXT collaboration which produced low spatial-resolution maps of the contamination – the deployment of humans equipped with hand-held dose-meters to manually measure radioactivity levels generates results at the highest possible spatial-resolution, though as would be anticipated, the coverage of this method is inherently

poor. Like the helicopter-based mapping however, such a measurement technique also exposes those who are undertaking the work to even more significant levels of ionising radiation as a result of their closeness to the emitting source. The subsequent deployment of vehicular-based mapping systems [6,7] into the affected regions allowed greater areas to be covered with operators experiencing less radioactive dose. Both foot-based and vehicle surveys however are limited (to varying degrees) to what is accessible due to either terrain or the road network respectively. An intermediary system to monitor contamination was provided through unmanned helicopters previously used across Japan.

Low-Altitude Monitoring

To provide a means of monitoring contamination at improved resolutions, whilst not exposing operators to radiological dose, in addition to not being restricted by either terrain or the local road network, a number of groups within Japan adapted miniaturised helicopters for radiation mapping [8–10]. Such platforms were formerly used extensively across agricultural areas for crop-dusting. When repurposed, the systems consisted of an unmanned helicopter weighing approximately 100 kg, typically equipped with three large-volume (6.5 kg) CsI detectors mounted under the platform – capable of operating for durations of up to 1.5 hours at velocities of 8 m/s. Restricted by practicality (overhead obstructions) to 80 m altitude, an area on the scale of several tens of kilometers could be mapped at a resolution of 80 m^2 per pixel.

Like the high-altitude monitoring performed by the manned helicopter missions, a correction of the radiation intensity measured at altitude to a standard height above ground (1 m in all cases) was performed following an exponential reduction in intensity with distance from the simulated point-source [9,10].

Although this monitoring method represents a marked improvement in resolution in comparison to other methods, exposing operators to little / no harmful ionising radiation, the on-ground detail is still not directly comparable to foot or vehicle-based systems. The application of multi-rotor unmanned systems capable at operating at altitudes of sub-80 m represents a powerful tool for radiological surveying not only in the aftermath of the FDNPP accident but at other nuclear and contaminated sites worldwide [11,12].

A comparison of the differing survey methods, their intrinsic properties, strengths and limitations are shown in Table. 1.

TABLE I: Comparison of the different aerial platforms and properties used in assessing the contamination released following the FDNPP incident.

	C12 / UK-1 (manned)	Ground Monitoring	Helicopter (unmanned)	Low-Altitude UAV
Altitude	>150 m	1 m	80 m	5 – 15 m
Spatial resolution	300 – 500 m	<1 m	80 m pixel	<1 m
Coverage	100's km's	km's	10's km's	km's
Cost	High	Low	Moderate	Low
Dose to operators	Moderate	High	Low	Low

METHOD

Unmanned Aerial Vehicle (UAV)

The unmanned aerial vehicle (UAV) used as part of this work was designed and constructed in-house at the University of Bristol (UK), based on a X8 configuration. Initial system testing configuration and deployments of the platform are described fully in previous works by the authors [11]. Unlike other existing aerial platforms, the X8 configuration of the unit, consisting of four sets of counter-rotating propellers affords a greater stability during operation (especially in environments with elevated winds or sudden gusts) and redundancy in the event of propeller / motor failure.

Weighing a total of 7.0 kg; 1.3 m in diameter and 0.5 m in height when fully assembled – the system was capable of total flight durations of 30 – 35 minutes on lithium polymer (LiPo) batteries, carrying its 0.5 kg radiation mapping system.

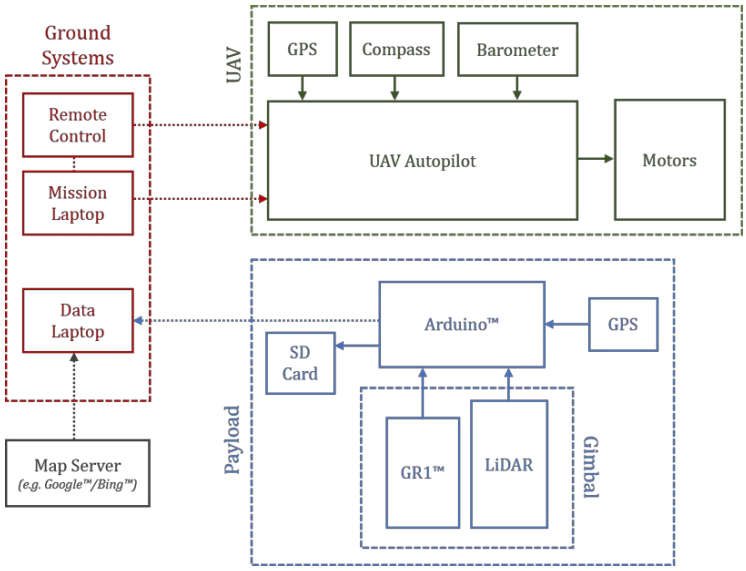

Fig. 1. Schematic of the UAV, radiation detection and associated ground-control system.

Radiation Detection and Quantification

Detection of incident radiation was performed through the use of a miniaturised gamma-ray spectrometer positioned on the underside of the UAV; alongside a single-point laser-rangefinder – both of which were mounted within an active gyroscopic gimbal to keep both pointing normal to the ground surface independent of the attitude of the UAV.

The gamma-ray spectrometer selected as the detector was a GR1 cadmium-zinc-telluride (CZT) detector from Kromek Ltd., weighing a total of 100 g, it possessed an active detection volume of 1 cm^3. With an energy range of 30 keV to 3 MeV, the maximum achievable count rate through the detector was 30,000 counts per second (CPS) across its 4096 channels (bins). Radiation incident onto the detector was recorded as a string on individual bins / gamma energies – with the total number of recorded representing the CPS value. The rangefinder used to determine the height above ground of the sensor system was an Acuity™ AR2500 time-of-flight based unit. The eye-safe infra-red unit has an accuracy of ±5 cm at 250 m, operating at a maximum sampling frequency of 30 kHz.

Custom-built data acquisition software was produced to sample from both the radiation detector and the rangefinder simultaneously; recording both data streams onto a micro-SD card contained within an Arduino™ microcontroller, alongside a GPS position sourced from a unit mounted within the detection payload. In order to monitor the data in real-time, live encrypted telemetry was broadcast back to a base station via a radio-frequency module.

To examine the application and assess the suitability of the low altitude UAV system for mapping radiation anomalies (and subsequent contaminant modelling), several test sites were selected across the contamination impacted Fukushima Prefecture. Location 1 was a tiered field formerly used for the subsistence production of rice prior to the incident located in Kawamata Town close to the border with Namie; it was assumed to be initially homogenously blanketed in contamination as a result of the radiological release. An extensive irrigation network existed surrounding the perimeter of the small fields that composed the elongate site. Location 2 (located to the north of Location 1) more centrally in the main NW trending plume-line within the village of Iitate, consisted of a number of small flat fields of differing crop-type, intersected by both a road and small river. The final location discussed, Location 3, was a former cattle farm, also located within Kawamata – on the border with the more heavily contaminated Namie Town to the east. This large agricultural field formed part of a Japanese Atomic Energy Agency test site to examine potential methods through which surface activity could be reduced.

Throughout this study, a consistent ground-equivalent flight speed of 1.5 m/s for the UAV was selected to ensure a suitable balance between both adequate ground coverage and spatial-resolution attainable (with measurements taken at a sampling frequency of 2 Hz). The altitude at which the system was operated at during each of the surveys was conversely not rigidly set, a typical survey height of 5 m was selected

where no obstructions (buildings and trees etc.) existed and the area was largely flat (Locations 2 and 3). For areas where obstructions existed and/or steep topography was encountered (Location 1), greater survey altitudes were employed (up to 20 m above the ground surface).

Data Analysis

To facilitate the analysis of the data collected via the UAV, custom software was constructed at the University of Bristol. Within this software, each location point (recorded as a longitude and latitude via the systems on-board GPS unit) was converted to a raw XYZ format for plotting. For each of these data points (or conversely a number of selected points), a gamma-ray spectrum could be constructed by summing each of the individual gamma energies measured as incident onto the detector. Using the altitude above ground value obtained from the single-point rangefinder mounted on the system, a normalisation of height to correspond to the radiation level 1 m above the ground was made.

In order to easily identify/represent regions of elevated contamination, a temperature-scaled coloured overlay onto a Google Earth™ base map was employed. Three-dimensional plots were also used to highlight areas across the survey region where radiation existed at raised levels. For subsequent analysis and interrogation of the results, the software also allowed for the results processed within the custom-built software to be exported in a number of differing formats for analysis within commercially-available graphic information software (GIS) packages (e.g. ArcGIS™ and ENVI™), graphical platforms (e.g. OriginLab™) or statistical analysis platforms (e.g. MatLab™ and R).

Contaminant Modelling

After conducting high spatial-resolution mapping at the contrasting localities detailed above using the UAV; subsequent modelling and predictive transport calculations were applied to some of the data obtained. In order to model the various potential factors contributing to dose-rate reduction over a time-resolved period, a number of factors were combined within a custom-written MatLab™ script. Within this script, the influence of the reduction in activity as a result of the natural decay of the radiocesium (Cs-134 and Cs-137) was combined with the potential effects of fluvial transport down-stream. Finally, the impact of the downward migration of the gamma-ray emitting species into the soil regolith was incorporated, with the inherent shielding of activity as a result. For this, the soil depth profiles examined in the works of Kato et al. (2012) [13], Ohno et al. (2012) [14] and Teramage et al. (2014) [15] were used.

RESULTS & DISCUSSION

Through the application of the UAV with associated radiation mapping system described above, highly-detailed maps showing the distribution of contamination

across each of the three localities are hereby presented below (Figs. 2 – 4). Operating at greatly reduced altitudes in comparison to other measurement methods, the results presented here show radiological anomalies at scale-lengths formerly unachievable through higher-altitude methods.

Location 1

By subtracting the altitude data derived from the systems on-board GPS unit from the height values obtained from the single-point rangefinder mounted within the payload, an approximation of the underlying surface topography can be produced. The result of this topographic approximation achieved via the UAV overflight are shown in Fig. 2 (a). Apparent are the small horizontal areas that constitute the individual rice fields, punctuated by the irrigation network. An elevated area to the west of the site (shown in red) is also evident. Using this point-cloud data – transferring the results into ArcGIS for manipulation, a triangular irregular network (TIN) was produced (Fig. 2 (b)); with this the radiation intensity data from the collection flights could be applied in order to yield a 3-dimensional radiation anomaly map.

From the results in Fig. 2 (b), as would be anticipated as a consequence of irrigation and meteoric events – there is the clear pre-concentration of radioactive material within a number of low-points across the site (shown as “thermal spots”). Assuming an initially homogeneous distribution of material following the 2011 event, specific positions are accumulating considerable radiative material.

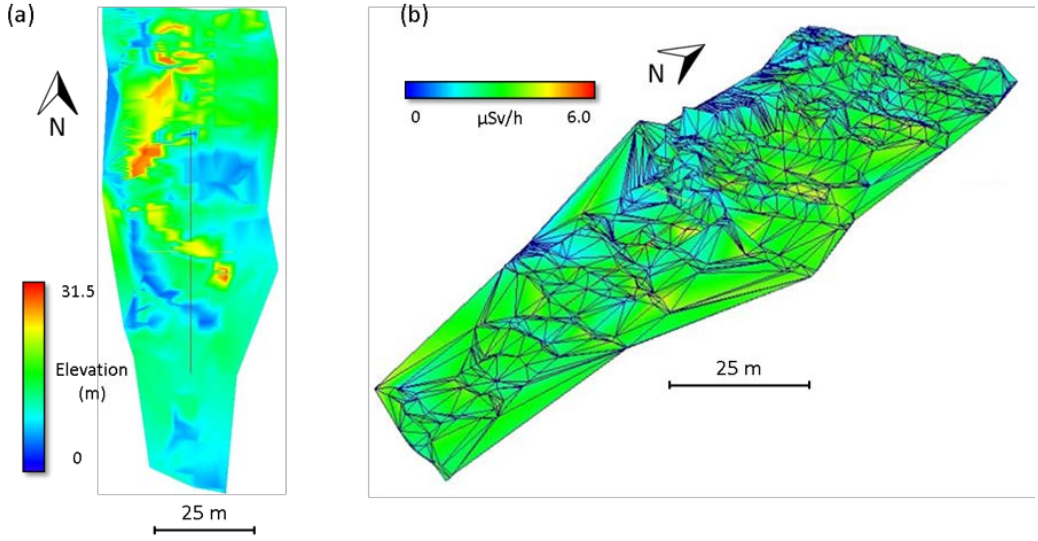

Fig. 2. 3-dimensional radiation survey generated by the unmanned platform; (a) detailed topographic map of Location 1 generated by comparison of GPS-derived altitude and distance from the rangefinder and (b) a triangular irregular network (TIN) overlain with the contamination measurements obtained.

Location 2

The results of time-resolved airborne radiation mapping performed at Location 2 during May 2014 and October 2015 are shown in Fig. 3. Apparent between the two surveys taken at 17-month separation is the reduction in dose-rate across the entirety of the site (from an average of 4.8 μSv/hr to 1.7 μSv/hr).

At the time of the initial radiological survey in May 2014, not remedial action had been performed on the site, with the difference in the dose-rate observed to the north and south of the transecting road being attributed to the differing crop species present. During the second survey, portions of the site had seen some remediation action (transecting road and a portion of the site to the far east), with some of this contaminated material being subsequently stored between this remediated area and the neighbouring road.

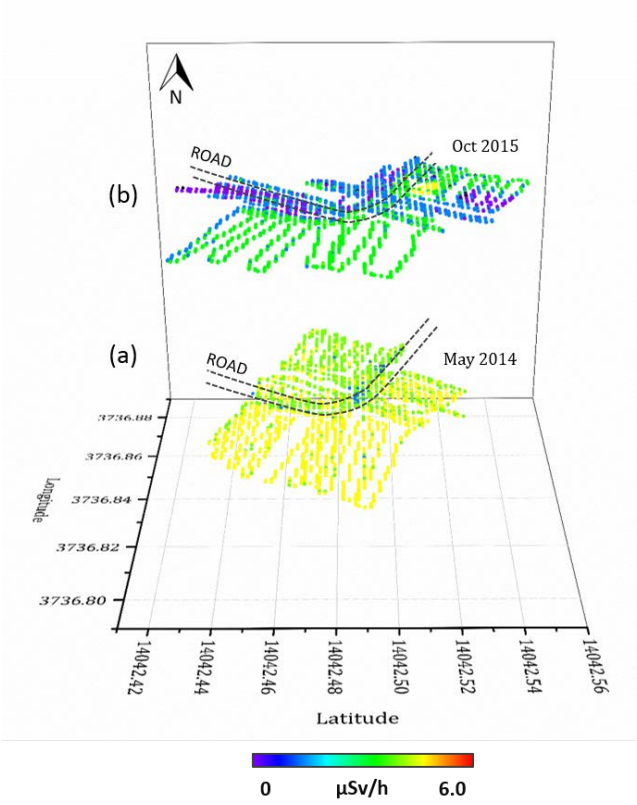

Fig. 3. Offset radiation intensity plots (dose-rate) produced from (a) May 2014 and (b) October 2015, with the location of the transecting road identified.

When this measured reduction in dose-rate between the two surveys (at 14 uninfluenced points across the site) is compared with the reduction that is predicted solely as a result of radioactive decay, a disparity however is observed to exist. This is shown graphically within Fig. 4., with the CPS value calculated to occur represented by the black bars, the value measured depicted by the red bars and the percentage

difference between the two indicated. Using the modelling method described above, (incorporating the influence of downwards migration on detected activity) it was determined that the discrepancy is a result of the transport of the particle-bound cesium away from the site by the river – eastwards into the neighbouring Pacific Ocean as suspended particle load.

Site 14 in Location 2; signifying an increase in the measured activity over what was calculated to exist represents the position on the Iitate Village site where the collected material was being stored as an interim measure before being transported off-site to the main waste storage facility nearby.

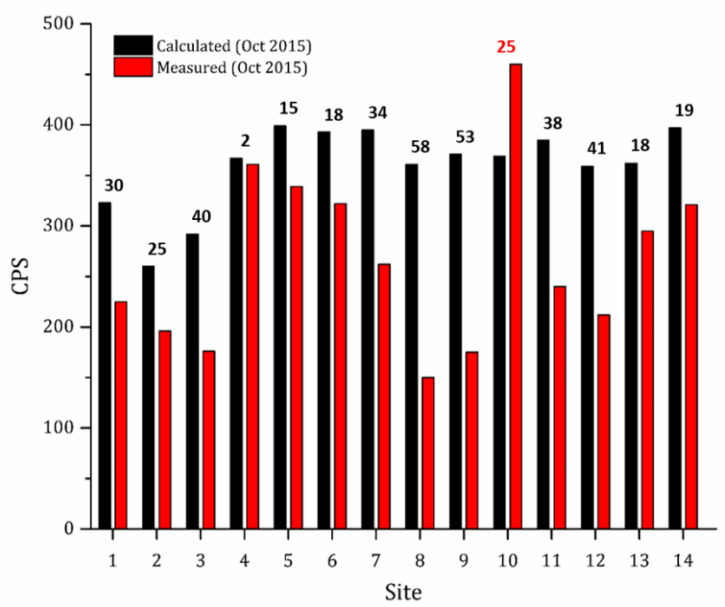

Fig. 4. Comparison of both measured and calculated readings from across the 14 selected sites for October 2015. The percentage difference between the two values (calculated and measured) is shown.

Location 3

The third locale studied to demonstrate the suitability of the UAV platform for high-spatial resolution radiation mapping was a JAEA test site located on the border with the heavily contaminated Namie Town. As part of the experiments conducted by the JAEA, a central circular region approximately 25 x 50 m was overlain with a thickness of sharp-sand,15 cm in thickness, to investigate the shielding that could be imparted on a homogenously contaminated area.

Results obtained by the UAV for Location 3 are presented in Fig. 5, with the outline perimeter of the sand covering marked. From this radiation map produced over the location, the difference in the measured intensity over the area that is overlain with

sand and that which is not is immediately apparent. The typical dose-rate obtained over the bare-field averages at 5 μSv/hr, whilst the corresponding dose-rate measured over the nearby sand shielded region being less than 50% of this value at only 2.3 μSv/hr.

A graphical representation of the effectiveness of this sand coverage is presented in Fig. 6 along the transect A – B (shown in Fig. 5). The effectiveness of this covering is highly-evident, with a rapid decline in measured count-rate over a very small transitional window. Whilst this method of reducing the above-ground dose-rate is seen to be effective, the practicality of depositing such a considerable volume of material is a matter of much debate – with the long-term effectiveness within such a physically and chemically intensive environment a potential issue.

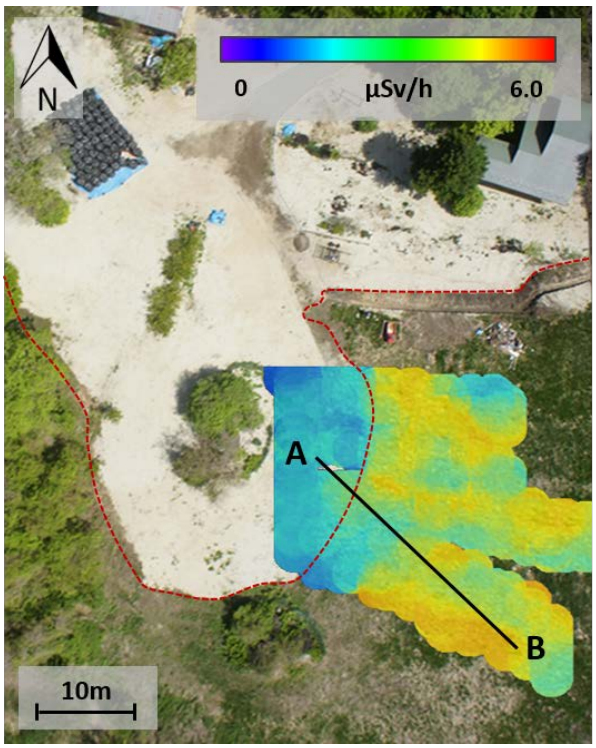

Fig. 5. Radiation map generated by the UAV showing the marked difference between the central (sand-covered region) and the uncovered surroundings. The transect (A – B) showing this change is presented graphically within Fig. 6 (below).

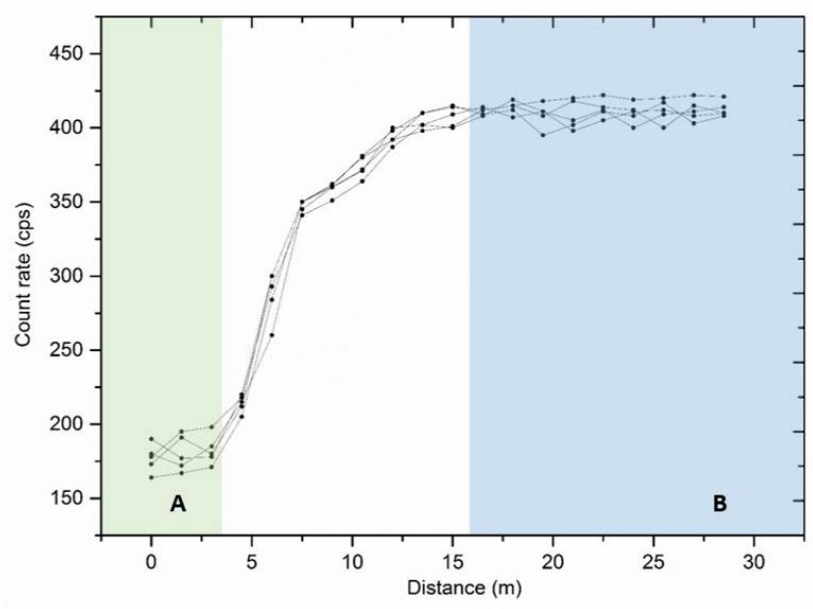

Fig. 6. Increase in activity observed from A to B (Fig. 5) from the sand covered (central) region outwards into the surrounding field.

CONCLUSIONS

Through the application of low altitude unmanned aerial vehicles (UAVs) to a number of test sites within the radiation affected Fukushima Prefecture, their potential to provide valuable high spatial-resolution data, without exposing those conducting the surveys to harmful radiation, is shown. The use of such systems represents an integral part of a comprehensive "toolkit" for the complete radiation mapping of a contaminated region across a range of length-scales and speeds. As well as being lightweight and easily deployable, the low-cost of such a platform has presented the potential for its application on the Sellafield Ltd. nuclear site in Cumbria (UK) on a number of selected exemplar surveys [16].

By collecting these highly-detailed radiation maps it was possible forward model the migration of radionuclides in the rapidly-evolving and dynamic Fukushima environment. Combined with the physical sampling and laboratory-based analysis of material derived from the region, a highly-comprehensive environmental account of the behaviour of ejecta species and the accident itself is achievable.

REFERENCES

1. Steinhauser, G.; Brandl, A.; Johnson, T. E. Comparison of the Chernobyl and Fukushima nuclear accidents: a review of the environmental impacts. *Sci. Total Environ.* **2014**, *470–471*, 800–817.

2. Bolsunovsky, A.; Dementyev, D. Evidence of the radioactive fallout in the center

of asia (Russia) following the fukushima nuclear accident. *J. Environ. Radioact.* **2011**, *102*, 1062–1064.

3. Lozano, R. L.; Hernández-Ceballos, M. A.; Adame, J. A.; Casas-Ruíz, M.; Sorribas, M.; Miguel, E. G. S.; Bolívar, J. P. Radioactive impact of Fukushima accident on the Iberian Peninsula: Evolution and plume previous pathway. *Environ. Int.* **2011**, *37*, 1259–1264.

4. Loaiza, P.; Brudanin, V.; Piquemal, F.; Reyss, J. L.; Stekl, I.; Warot, G.; Zampaolo, M. Air radioactivity levels following the Fukushima reactor accident measured at the Laboratoire Souterrain de Modane, France. *J. Environ. Radioact.* **2012**, *114*, 66–70.

5. Le Petit, G.; Douysset, G.; Ducros, G.; Gross, P.; Achim, P.; Monfort, M.; Raymond, P.; Pontillon, Y.; Jutier, C.; Blanchard, X.; Taffary, T.; Moulin, C. Analysis of Radionuclide Releases from the Fukushima Dai-Ichi Nuclear Power Plant Accident Part I. *Pure Appl. Geophys.* **2012**, *171*, 629–644.

6. Ikuta, M.; Gobara, H.; Tanaka, A.; Kimura, K. Car-Borne Survey Using Ge Semiconductor Detector in the Chugoku Region of Japan. *Japanese J. Heal. Phys.* **2012**, *47*, 198–203.

7. Tsuda, S.; Yoshida, T.; Sato, T.; Seki, A.; Matsuda, N.; Ando, M.; Saito, K.; Nakahara, Y.; Takemiya, H.; Tanigaki, M.; Takamiya, K.; Sato, N.; Okumura, R.; Kobayashi, Y.; Yoshinaga, H.; Yoshino, H.; Uchihori, Y.; Ishikawa, M.; Iwaoka, K. Construction of a car-borne survey system for measurement of dose rates in air. KURAMA-II, and its application. *JAEA Technol.* **2013**, *2013–37*, 68.

8. Sanada, Y.; Kondo, A.; Sugita, T.; Torii, T. Distribution of radioactive cesium measured by aerial radiation monitoring. *Hoshasen* **2012**, *38 (3)*, 137–140.

9. Sanada, Y.; Kondo, A.; Sugita, T.; Nishizawa, Y.; Youichi, Y.; Kazutaka, I.; Yasunori, S.; Torii, T. Radiation monitoring using an unmanned helicopter in the evacuation zone around the Fukushima Daiichi nuclear power plant. *Explor. Geophys.* **2014**.

10. Sanada, Y.; Torii, T. Aerial radiation monitoring around the Fukushima Dai-ichi Nuclear Power Plant using an unmanned helicopter. *J. Environ. Radioact.* **2015**, *139*, 294–9.

11. Martin, P. G.; Payton, O. D.; Fardoulis, J. S.; Richards, D. A.; Scott, T. B. The use of unmanned aerial systems for the mapping of legacy uranium mines. *J. Environ. Radioact.* **2015**, *143*, 135–140.

12. Martin, P. G.; Payton, O. D.; Fardoulis, J. S.; Richards, D. A.; Yamashiki, Y.; Scott, T. B. Low altitude unmanned aerial vehicle for characterising remediation effectiveness following the FDNPP accident. *J. Environ. Radioact.* **2016**, *151*, 58–63.

13. Kato, H.; Onda, Y.; Teramage, M. Depth distribution of 137Cs, 134Cs, and 131I in soil profile after Fukushima Dai-ichi Nuclear Power Plant Accident. *J. Environ. Radioact.* **2012**, *111*, 59–64.

14. Ohno, T.; Muramatsu, Y.; Miura, Y.; Oda, K.; Inagawa, N.; Ogawa, H.; Yamazaki, A.; Toyama, C.; Sato, M. Depth profiles of radioactive cesium and iodine released

from the Fukushima Daiichi nuclear power plant in different agricultural fields and forests. *Geochem. J.* **2012**, *46*, 287–295.

15. Teramage, M. T.; Onda, Y.; Patin, J.; Kato, H.; Gomi, T.; Nam, S. Vertical distribution of radiocesium in coniferous forest soil after the Fukushima nuclear power plant accident. *J. Environ. Radioact.* **2014**, *137*, 37–45.

16. Martin, P. G.; Moore, J.; Fardoulis, J. S.; Payton, O. D.; Scott, T. B. Radiological Assessment on Interest Areas on the Sellafield Nuclear Site via Unmanned Aerial Vehicle. *Remote Sens.* **2016**, *8*, 913.

ACKNOWLEDGEMENTS

This work was funded as part of the University of Bristol and Kyoto University Strategic Alliance, with additional support provided by the EPSRC, Kromek Ltd., Sellafield Ltd., AWE (UK) as well as the University of Bristol's Cabot Institute and Alumni Foundation. The authors wish to acknowledge the University of Bristol School of Physics Workshop for their assistance in the construction of the airframe used in this work.